He et al. Nanoscale Research Letters (2016) 11:330
DOI 10.1186/s11671-016-1550-2

Nanoscale Research Letters

NANO EXPRESS Open Access

Structural Properties and Phase Transition of Na Adsorption on Monolayer MoS_2

Hai He[1], Pengfei Lu[1,3*], Liyuan Wu[1], Chunfang Zhang[2], Yuxin Song[3], Pengfei Guan[2*] and Shumin Wang[3,4]

Abstract

First-principles calculations are performed to investigate the structural stability of Na adsorption on 1H and 1T phases of monolayer MoS_2. Our results demonstrate that it is likely to make the stability of distorted 1T phase of MoS_2 over the 1H phase through adsorption of Na atoms. The type of distortion depends on the concentration of adsorbed Na atoms and changes from zigzag-like to diamond-like with the increasing of adsorbed Na atom concentrations. Our calculations show that the phase transition from 1H-MoS_2 to 1T-MoS_2 can be obtained by Na adsorption. We also calculate the electrochemical properties of Na adsorption on MoS_2 monolayer. These results indicate that MoS_2 is one of potential negative electrodes for Na-ion batteries.

Keywords: First-principles, MoS_2, Structural stability, Phase transition

Background

In recent years, the study of transition-metal dichalcogenides (TMDs) has been a topic of current interest due to their layered structure [1, 2]. TMDs exhibit a broad range of properties, which are advantageous for a wide range of applications as high-performance functional nanomaterials [3]. Among them, molybdenum disulfide (MoS_2) has attracted considerable attention because of its important role in ultrasensitive photodetectors, flexible electronic device, lithium ion battery, field effect transistors, and sodium-ion batteries [4–7]. These applications show high figure of merit in microelectronics, thermoelectrics, and optoelectronics.

Bulk MoS_2 crystal is an indirect-gap semiconductor, which is built up of atomic layers stacking by weak van der Waals force. It is possible to exfoliate MoS_2 monolayer from the bulk, owing to the weak van der Waals interaction between these layers [8, 9]. The typical monolayers of TMDs come in two varieties, called H and T phase with trigonal or octahedral prismatic coordination, respectively [10]. Consequently, MoS_2 monolayers come in two phases, called 1H-MoS_2 and 1T-MoS_2 [11]. The 1H-MoS_2 phase has the space group of P6/mmc and is semiconducting with a direct band gap [12]. The 1T-MoS_2 phase is metallic and metastable relative to the 1H-MoS_2 phase [13]. However, stable 1T-MoS_2 phase can be realized by doping of MoS_2 with Re atoms [14] and be stabilized by adsorption of Li atoms [15].

Previous studies demonstrated the phase transition between 1H-MoS_2 and 1T-MoS_2 in the early lithiation process [16–20]. The charge transfer induced by the adatoms leads to turn 1T-MoS_2 phase into a stable MoS_2 phase. The phase transition is the main issue for application in Li-ion batteries [20, 21] and Na-ion batteries [22, 23]. A large amount of experimental and theoretical works on the application of MoS_2 in Li-ion batteries has emerged in the past years [16–21]. Kan et al. [16] studied possible pathways of structural phase transition between 1H-MoS_2 and 1T-MoS_2 by increasing lithium adsorption concentration constantly. Esfahani et al. [18] calculated the H-T transition by adsorption of Li atoms on both sides of the MoS_2 monolayer. Mortazavi et al. [22] investigated phase transition between 2H-MoS_2 and 1T-MoS_2 upon Na intercalation. Li-ion batteries are prime energy storage systems at present in amounts of devices used in our daily lives such as smartphones and laptops. Na-ion batteries are excellent alternatives to Li-ion batteries because of their lower cost and the greater availability. However,

* Correspondence: photon.bupt@gmail.com; pguan@csrc.ac.cn
[1]State Key Laboratory of Information Photonics and Optical Communications, Ministry of Education, Beijing University of Posts and Telecommunications, PO Box 72, Beijing 100876, China
[2]Beijing Computational Science Research Center, Beijing 100084, China
Full list of author information is available at the end of the article

to our knowledge, there are few theoretical calculations on Na adsorption on monolayer MoS_2.

In this work, we perform a comprehensive first-principles study of the electronic structure, adsorption energies, phase transitions, and electrochemical properties for Na-adsorption compounds. All reasonable structure phases of MoS_2 monolayer are introduced. Our results suggest that it is easily to turn to be octahedral phases by Na-adsorption for 1T-MoS_2, such as ZT-MoS_2 with zigzag Mo-Mo chains and DT-MoS_2 in rhombus-shape with Mo-Mo chains. Furthermore, Na adsorption on the MoS_2 surface can lead to a structural phase transformation from 1H-MoS_2 to an octahedral coordinated MoS_2. Average operating voltages by Na adsorption are calculated. This will be helpful to understand the basic processes involved in monolayer MoS_2 applied in Na-ion batteries.

Methods

Our calculations are carried out by using the Vienna Ab-initio Simulation Package (VASP) package [24], which is based on density functional theory (DFT) and plane-wave pseudopotential method. The electron exchange-correlation energy is described in the Perdew-Burke-Ernzerhof (PBE) form for the generalized gradient approximation (GGA) [25]. The cut-off energy is set to be 600 eV for the plane-wave expansion of the wave functions. The Brillouin zone integration is represented by the Monkhorst-Pack k-point scheme with $9 \times 9 \times 1$ and $5 \times 5 \times 1$ grid meshes for the (1×1) unit cell and (4×4) supercell, respectively. The criterion of convergence of energy is chosen as 10^{-5} eV between two ionic steps, and the maximum force allowed on each atom is 0.01 eV/Å. The vacuum space along the z direction is taken to be more than 15 Å for the both 1H-MoS_2 and 1T-MoS_2.

The geometry structures are shown in Fig. 1. A (4×4) supercell of MoS_2 monolayer consisting of 48 atoms, which contains 16 Mo and 32 S, is made up of the primitive cell of MoS_2. 1H-MoS_2 has single S-Mo-S layer, where the Mo site in a trigonal prism coordination as shown in Fig. 1a. 1T-MoS_2 has asymmetric sulphur atoms sites, where the Mo site in octahedral coordination as shown in Fig. 1b.

Results and Discussion

Structural Properties

To obtain a clear insight into the 1H to 1T phase transition, we first calculate electronic structures of both the trigonal prismatic phase (1H-MoS_2) and octahedral prismatic phase (1T-MoS_2) by using (1×1) unit cell. Our results show that the optimized lattice parameters a_0 = 3.166 Å for both the pristine 1H-MoS_2 and the pristine 1T-MoS_2 as shown in Table 1.

Electronic structure provides a clear insight into the difference of band structure between 1H-MoS_2 and 1T-MoS_2. The two phases show completely different electronic structures. Figure 2 shows the band structures of 1H-MoS_2 and 1T-MoS_2 without spin-orbit coupling. 1H-MoS_2 is a direct semiconductor with both conduction band minimum (CBM) and valence band maximum (VBM) located at the K point. The band gap obtained from GGA-PBE calculations is 1.71 eV. However, the electronic structure calculation of the 1T structure shows that this polytype is indeed metallic in Fig. 2b. We also calculate the energy difference between 1H-MoS_2 and undistorted 1T-MoS_2 unit cell, which shows that the optimized 1H-MoS_2 is more stable than the 1T-MoS_2 by 0.84 eV. In normal conditions, although both polytypes of monolayer MoS_2 have the same element constitution, 1H-MoS_2 is more stable than 1T-MoS_2. Besides, the equilibrium lattice constant of 1H-MoS_2 is close to that of 1T-MoS_2 according to Table 1.

Adsorption Energies and Stability Analysis

In order to investigate the stability of the two structural phases with Na adsorption, the most stable configuration of an isolated Na atom adsorbed on (4×4) cell for the both structure phases is determined at first. Three different types of adsorption sites are introduced to

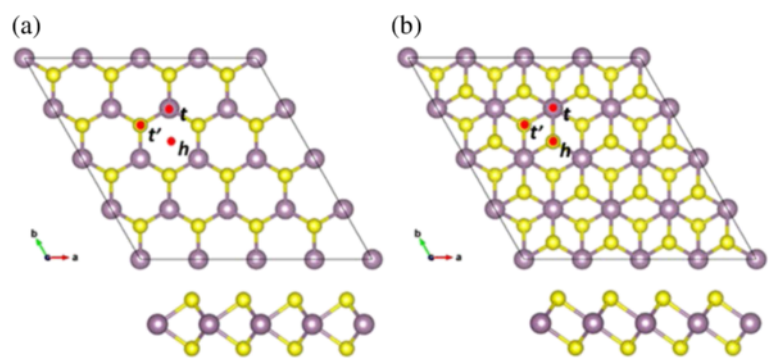

Fig. 1 **a** Top and side views of 1H-MoS_2. **b** Top and side views of 1T-MoS_2

Table 1 Structural parameters of 1H-MoS_2 and 1T-MoS_2 and band gap

		1H-MoS_2	1T-MoS_2
a (Å)	Present work	3.166	3.168
	References	3.16 [30]; 3.18 [11]	3.18 [10]
$d_{S\text{-}S}$ (Å)	Present work	3.092	3.092
	References	3.089 [30]	–
Gap (eV)	Present work	1.71	Metal
	References	1.71 [30]; 1.67 [11]	Metal

determine the most stable position [26], including "t" site (top site directly above a Mo atom), t' site (top site directly above an S atom), and "h" site (hollow site above the center of hexagons), respectively. Na atoms adsorbed at other positions can eventually relax into one of the three listed adsorption sites [27]. Considering the monolayer hexagonal lattice structure of MoS_2 monolayer, it is reasonable to expect the relaxation of foreign atoms on one of these adsorption sites. There is little change for the adsorption geometry of 1H-MoS_2 after relaxation. However, the optimized 1T-MoS_2 supercell will transform into the distorted 1T phase duo to its instability, such as ZT-MoS_2 with zigzag Mo-Mo chains. Further, to investigate the relative stabilities of the systems, we defined the adsorption energy as follows:

$$E_a = (E_{X-\mathrm{MoS2}} + E_{\mathrm{Na}}) - E^x_{\mathrm{total}} \quad (1)$$

where X = 1H, distorted 1T, $E_{X-\mathrm{MoS2}}$ represents the total energy of 1H-MoS_2 and distorted 1T-MoS_2 system, E^x_{total} represents the total energy of the adsorption system, and E_{Na} represents the total energy of bulk sodium. The electron configurations of adatom adsorption energies (E_a) and structural properties for single adatom-adsorbed MoS_2 obtained from our calculations are listed in Table 2. Our calculated results show that the adsorption energy is different for different sites. In all adsorption sites, the site with the largest adsorption energy (minimum total energy) is referred to as the favored one. Comparing the possible sites of h, t, and t', we found that Na atom prefer to reside on t site for the both structures.

Phase Transition of 2D MoS_2 Monolayer Induced by Na Insertion

In the previous analysis, we have determined the most stable adsorption site for Na atoms on the surface of MoS_2 monolayer, which is top of Mo atom sites. Totally, there are 32 most stable sites for Na atoms on both sides of (4×4) MoS_2 supercell [28]. In order to investigate systematically Na adsorption on the surface of MoS_2 monolayer, we introduce Na atoms on both sides of MoS_2 monolayer forming the compound 1H-Na_xMoS_2 and 1T-Na_xMoS_2 to induce phase transition, which is a solvent-based exfoliation of MoS_2 monolayer and a typical procedure for both the charge/discharge processes in battery.

The geometries of 1H-Na_xMoS_2 are optimized with adsorption concentration increasing, as shown in Fig. 3. Our results show the variation of energies and structure for 1H-Na_xMoS_2 with the increasing of Na concentrations. As shown in Fig. 3, Mo-Mo chains appear in 1H-Na_xMoS_2 when 2~6 Na atoms are added to the system.

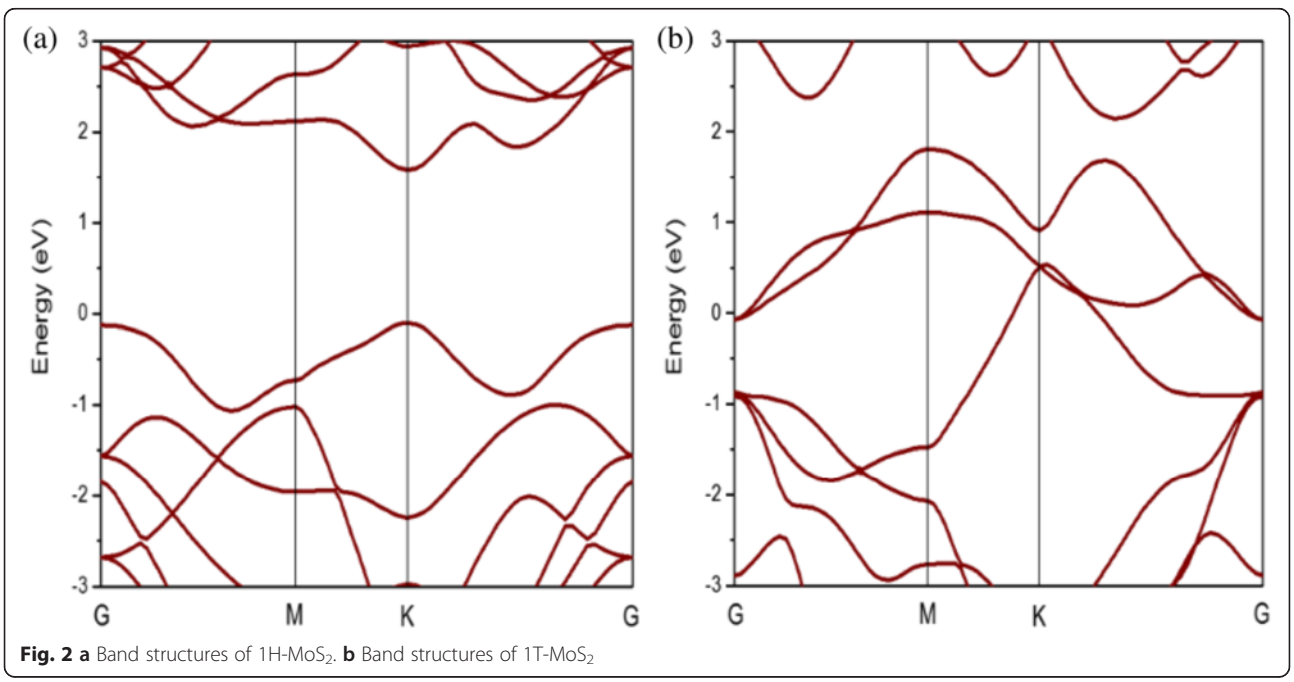

Fig. 2 **a** Band structures of 1H-MoS_2. **b** Band structures of 1T-MoS_2

Table 2 Adsorption energy, distance between Na and S atoms, the bond length of Mo-Mo

	Site	E_a (eV)	$d_{Na\text{-}S}$ (Å)	$d_{Mo\text{-}Mo}$ (Å)
1H-MoS_2	h	2.1	2.74	2.97
	t′	3.2	2.68	3.04
	t	1.8	2.76	3.02
Distorted 1T-MoS_2	h	2.7	2.75	2.89
	t′	3.6	2.66	2.92
	t	2.3	2.76	2.93

Triangular Mo-Mo clustering appears in 1H-Na_xMoS_2 with the increasing of adsorption concentrations.

The optimized geometries of 1T-Na_xMoS_2 with the increasing of adsorption concentrations are shown in Fig. 4a. The substrate structure of 1T-MoS_2 directly transits to the ZT-MoS_2 after relaxation due to the instability. Some Mo-Mo chains appear in 1T-Na_xMoS_2 following certain rules. These Mo atoms gradually form a diamond-like chain up to eight Na atoms that are introduced in the system. The system is likely to maintain the diamond chain structure. The geometry configurations of ZT-MoS_2 and DT-MoS_2 without adsorption are clearly shown in Fig. 4b, c, respectively. The free-standing 1T-MoS_2 exhibits metallic property and is metastable. Both ZT-MoS_2 and DT-MoS_2 belong to distorted octahedral coordinated MoS_2.

It is similar to the definition of adsorption energy that the formation energy in different concentrations of Na absorption is calculated using the expression:

$$E_{f(x)} = E_{(X-\mathrm{Na}x\mathrm{MoS2})} - E_{(X-\mathrm{MoS2})} - nE_{(\mathrm{Na})} \quad (2)$$

where X = 1H, 1T, $E_{(X-\mathrm{Na}x\mathrm{MoS2})}$ is the total energy of the X-Na_xMoS_2 compound, $E_{(\mathrm{MoS2})}$ is the total energy of the same MoS_2 polytype, and $E_{(\mathrm{Na})}$ is the total energy of bulk sodium. A negative binding energy indicates an exothermic chemical interaction between Na and MoS_2. Relative formation energy per Na atom of 1T-Na_xMoS_2 with respect to 1H-Na_xMoS_2 varies as increasing the Na-adsorption concentration constantly in Fig. 5. The 1H-Na_xMoS_2 still keeps stability in the low adsorption concentration. However, the 1T-Na_xMoS_2 becomes more stable than 1H-Na_xMoS_2 when the adsorption concentration of Na atoms exceeds about 35 %. As the adsorption concentration of Na increases, the 1T-Na_xMoS_2 will become stable further.

Transition Barrier from 1H Phase to 1T Phase

The procedure of transition can be viewed as a shift of one S atom layer in the 1H-MoS_2 structure to the position h in Fig. 1a. Therefore, the barrier energy of 1H-MoS_2 structure to 1T-MoS_2 structure transition is able to be calculated by shearing one S layer from the

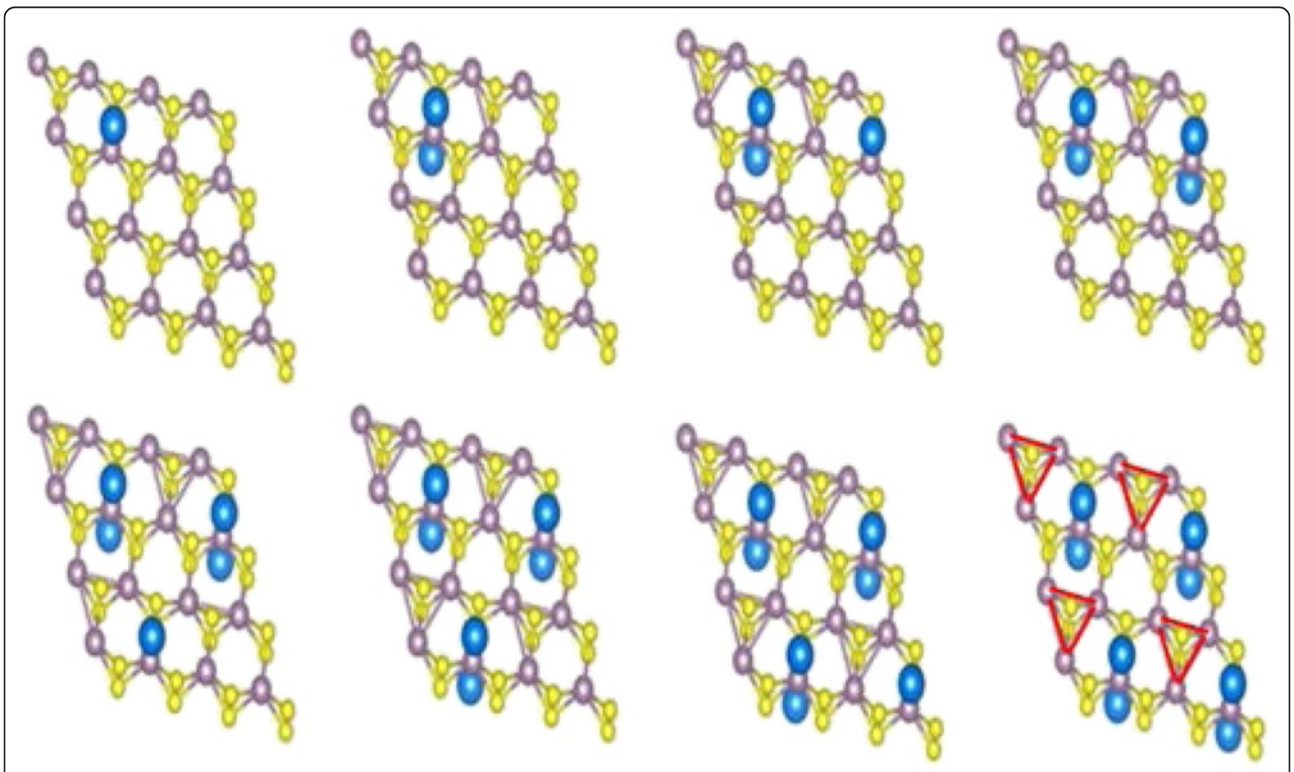

Fig. 3 The optimized structures of the most stable 1H-Na_xMoS_2, triangular Mo-Mo clustering as highlighted in *red*

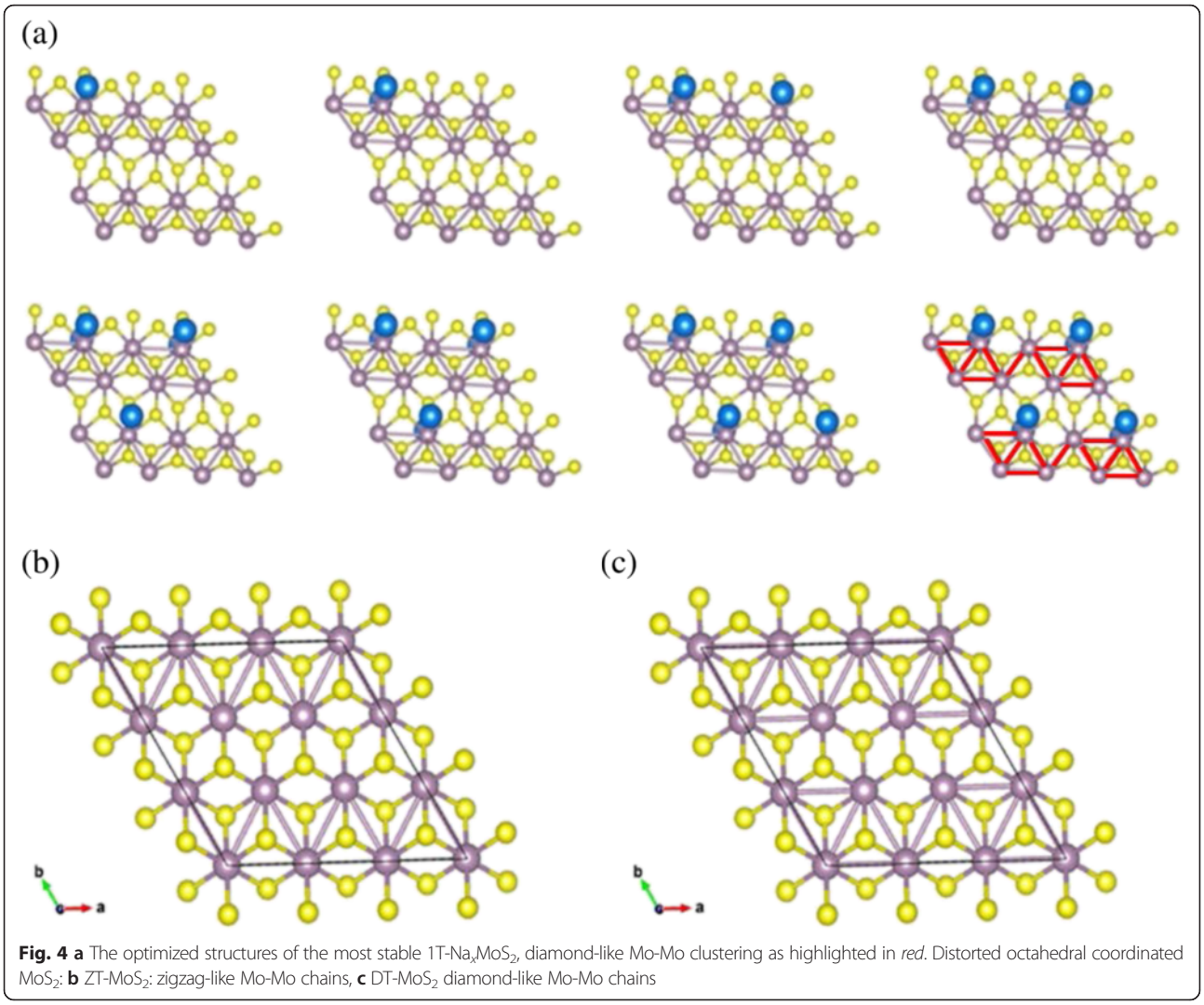

Fig. 4 a The optimized structures of the most stable 1T-Na_xMoS_2, diamond-like Mo-Mo clustering as highlighted in *red*. Distorted octahedral coordinated MoS_2: **b** ZT-MoS_2: zigzag-like Mo-Mo chains, **c** DT-MoS_2 diamond-like Mo-Mo chains

1H structure toward the 1T structure when fixing the Mo atoms, while the other atoms are allowed to relax. Nudged Elastic Band (NEB) method is adopted to calculate the barrier energy from 1H to 1T structure transition as shown in Fig. 6a. Our results show that the barrier of phase transition from 1H to 1T structure is approximately 1.61 eV in the absence of external adatoms. The phase transition involves one of the S atoms moving from one pyramidal position to the other pyramidal position. The relative energy of Na-intercalated 1T-MoS_2 is 0.52 eV. Meanwhile, the barrier from 1H-MoS_2 to 1T-MoS_2 reduces to 0.91 eV when Na atoms are adsorbed completely on one side of MoS_2 monolayer. The barrier energy reduces considerably from 1H to 1T structure transition by the Na atom adsorption on MoS_2 monolayer. These results suggest that the Na atoms are not only effective to make the 1T-MoS_2 energetically favorable but also play an important role in the process of phase transition. According to our theoretical calculation and experimental works, we summarize the pathways for structural phase transition among different structures in Fig. 6b. The detailed process is the following: (1) When Na atoms are adsorbed to 1H-MoS_2, the 1H-MoS_2 remains stable until the Na concentration reaches 35 %. When more Na atoms are adsorbed on both sides of MoS_2 monolayer, the distorted 1T-MoS_2 will become more stable. Besides, the structure finally transform to the distorted 1T-MoS_2 phase with diamond-like chains. (2) When all of the Na atoms are extracted from the system, the structure will become ZT-MoS_2. (3) The ZT-MoS_2 will transform back to 1H-MoS_2 phase by heating or aging.

Electrochemical Properties of Na_xMoS_2

In order to inspect the suitability of Na_xMoS_2 compound as an electrode material for Na-ions, we calculate the average adsorption voltage. The electrode

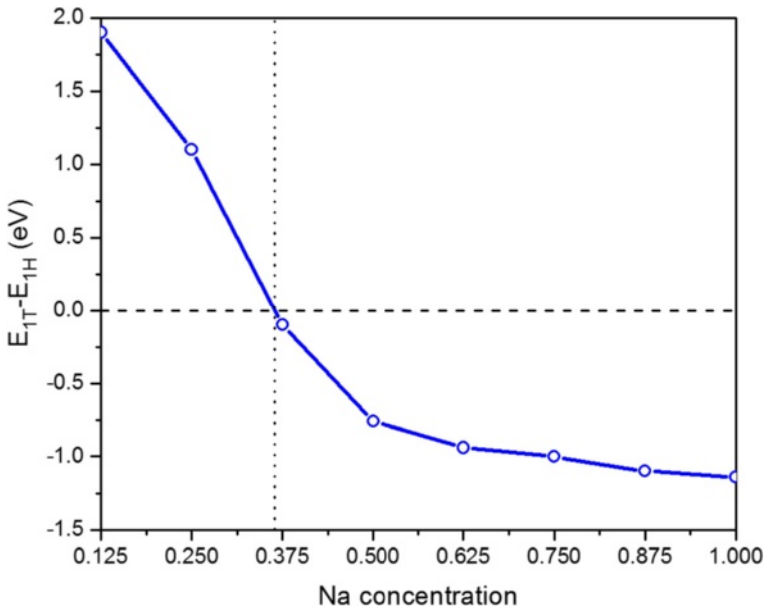

Fig. 5 Relative formation energy per Na atom of 1T-Na_xMoS_2 with respect to 1H-Na_xMoS_2 as a function of Na concentration

potential between $Na_{x1}MoS_2$ and $Na_{x2}MoS_2$ $(x_2 > x_1)$ is calculated as [29]:

$$\bar{V} = -\frac{G_{x_2} - G_{x_1} - (x_2 - x_1)G_{Na}}{(x_2 - x_1)e} \quad (3)$$

where G_{x_2} and G_{x_1} are the total energies of Na_xMoS_2 systems and G_{Na} is the energy per atom of Na in its bulk state. The electrode potential for 1H-Na_xMoS_2 and 1T-Na_xMoS_2 as the change of concentration is shown in Fig. 7, respectively. Our results show that the voltage profile for 1H-Na_xMoS_2 varies with a decreasing trend in a range of 0~1 V as shown in Fig. 7a, with an average value of 0.72 V. The electrode potential for 1T-Na_xMoS_2 varies in a range of 0~3.5 V as shown in Fig. 7b. However, 1T-Na_xMoS_2 systems are unstable for concentrations $x < 0.35$, as shown in Fig. 5. Therefore, the large magnitudes of the potential of 1T-Na_xMoS_2 compounds for low concentrations are unlikely to use practically. Our results show that the average potential of 1T-Na_xMoS_2 is obtained approximately as 1.28 V. Compared with Li-intercalated MoS_2, the average potential of Na_xMoS_2 is much lower because of the weaker binding of Na atoms. Since ideally a good anode should have a low electrode potential, our calculated voltage profile suggests that layered MoS_2 is suitable as an anode for an

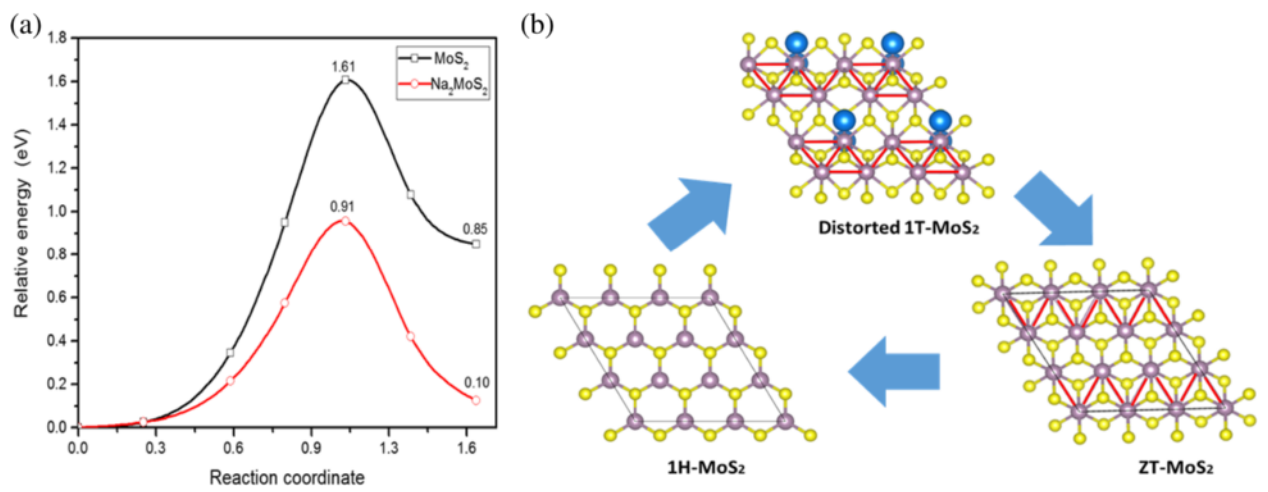

Fig. 6 a Evolution of the energy per S atom for 1H to 1T structure transition as a function of the reaction coordinate, for pure and Na-covered MoS_2. **b** The pathways of structural phase transition of Na adsorption on monolayer MoS_2

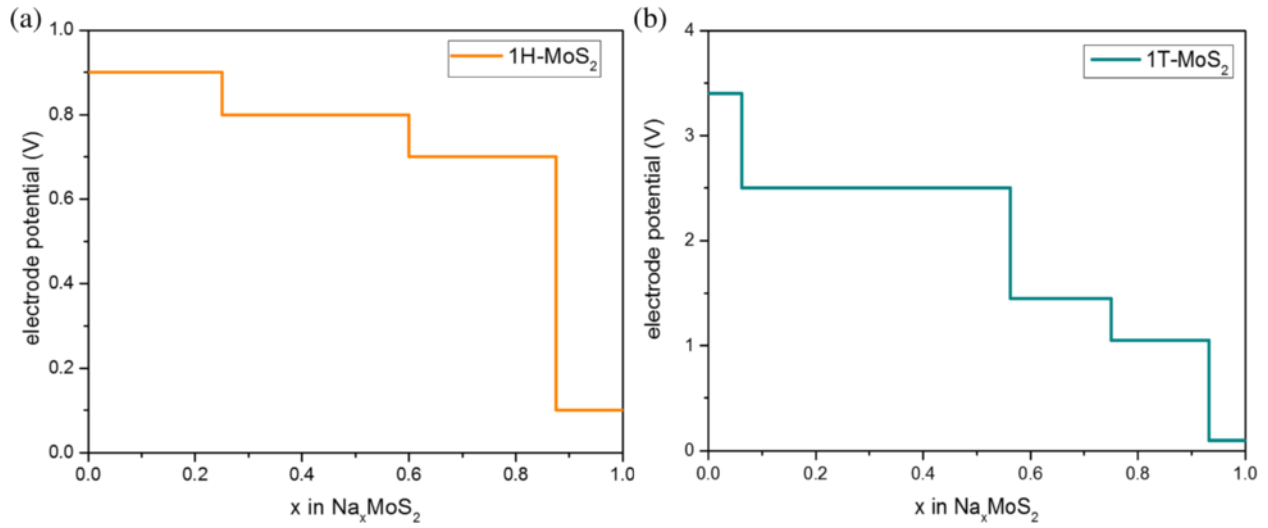

Fig. 7 Electrode potential of Na-intercalated **a** 1H-MoS_2 and **b** 1T-MoS_2

NIB. When this Na-intercalated MoS_2 anode is combined with high-capacity cathode materials such as $Na_3MnPO_4CO_3$, the Na-ion battery cell can yield a desirable open circuit voltage in the range of 2.5~3.5 V.

Conclusions

In conclusion, we investigated the adsorption energies, phase transition for the adsorption of Na onto MoS_2 monolayer, and electrochemical properties of Na_xMoS_2 by using the first-principles DFT method. The traditional trigonal prismatic 1H-MoS_2 phase is stable under normal conditions. However, a comprehensive study of the relative phase stability of MoS_2 tells us that the other structural phase transition can be stable by adsorption. Our results show that some triangular Mo-Mo clustering appears in 1H-Na_xMoS_2 with the increasing of Na-adsorption concentration. On the other hand, some diamond-like Mo-Mo chains appear in 1H-Na_xMoS_2 when the Na-adsorption concentration is beyond 25 %. What is more, the adsorption of Na on MoS_2 induces a phase transformation at $x = 0.35$ from the 1H to 1T phase. Our calculated results show that the adsorption of Na onto MoS_2 monolayer results in a lower energy barrier from 1H to 1T-MoS_2. Finally, Na_xMoS_2 compound is likely to become a battery anode material with a low average electrode potential of 0.72~1.28 V.

Acknowledgements

This work was supported by the National Basic Research Program of China (973 Program) under Grant No. 2014CB643900, the Open Fund of IPOC (BUPT), the Open Program of State Key Laboratory of Functional Materials for Informatics, the National Natural Science Foundation of China (No. 61404153), and the Shanghai Pujiang Program (Grant No.14PJ1410600). P.F. Guan acknowledges the computational support from the Beijing Computational Science Research Center (CSRC).

Authors' Contributions

HH carried out the calculations and HH and PFL wrote the manuscript. LYW, CFZ, YXS, and SMW helped in the discussions and analysis of the results. PFL and PFG proposed the initial work, supervised the analysis, and revised the manuscript. All authors read and approved the final manuscript.

Competing Interests

The authors declare that they have no competing interests.

Author details

[1]State Key Laboratory of Information Photonics and Optical Communications, Ministry of Education, Beijing University of Posts and Telecommunications, PO Box 72, Beijing 100876, China. [2]Beijing Computational Science Research Center, Beijing 100084, China. [3]State Key Laboratory of Functional Materials for Informatics, Shanghai Institute of Microsystem and Information Technology, Chinese Academy of Sciences, Shanghai 200050, China. [4]Photonics Laboratory, Department of Microtechnology and Nanoscience, Chalmers University of Technology, 41296 Gothenburg, Sweden.

Received: 1 June 2016 Accepted: 7 July 2016
Published online: 15 July 2016

References

1. Komsa HP, Krasheninnikov AV (2013) Electronic structures and optical properties of realistic transition metal dichalcogenide heterostructures from first principles. Phys Rev B 88(8):085318
2. Pandey M, Vojvodic A, Thygesen KS, Jacobsen KW (2015) Two-dimensional metal dichalcogenides and oxides for hydrogen evolution: a computational screening approach. J Phys Chem Lett 6(9):1577–1585
3. Kang J, Tongay S, Zhou J, Li J, Wu J (2013) Band offsets and heterostructures of two-dimensional semiconductors. Appl Phys Lett 102(1):012111
4. Baugher BW, Churchill HO, Yang Y, Jarillo-Herrero P (2013) Intrinsic electronic transport properties of high-quality monolayer and bilayer MoS_2. Nano Lett 13(9):4212–4216
5. Lopez-Sanchez O, Lembke D, Kayci M, Radenovic A, Kis A (2013) Ultrasensitive photodetectors based on monolayer MoS_2. Nat Nanotechnol 8(7):497–501
6. Wang S, Tu J, Yuan Y, Ma R, Jiao S (2016) Sodium modified molybdenum sulfide via molten salt electrolysis as an anode material for high performance sodium-ion batteries. Phys Chem Chem Phys 18(4):3204–3213
7. Yang E, Ji H, Jung Y (2015) Two-dimensional transition metal dichalcogenide monolayers as promising sodium ion battery anodes. J Phys Chem C 119(47): 26374–26380

8. Komsa HP, Krasheninnikov AV (2012) Effects of confinement and environment on the electronic structure and exciton binding energy of MoS_2 from first principles. Phys Rev B 86(24):241201
9. Lee C, Li Q, Kalb W, Liu XZ, Berger H, Carpick RW, Hone J (2010) Frictional characteristics of atomically thin sheets. Science 328(5974):76–80
10. Gordon RA, Yang D, Crozier ED, Jiang DT, Frindt RF (2002) Structures of exfoliated single layers of WS_2, MoS_2, and $MoSe_2$ in aqueous suspension. Phys Rev B 65(12):125407
11. Fan XL, Yang Y, Xiao P, Lau WM (2014) Site-specific catalytic activity in exfoliated MoS_2 single-layer polytypes for hydrogen evolution: basal plane and edges. J Mater Chem A 2(48):20545–20551
12. Kadantsev ES, Hawrylak P (2012) Electronic structure of a single MoS_2 monolayer. Solid State Commun 152(10):909–913
13. Calandra M (2013) Chemically exfoliated single-layer MoS_2: stability, lattice dynamics, and catalytic adsorption from first principles. Phys Rev B 88(24): 245428
14. Enyashin AN, Yadgarov L, Houben L, Popov I, Weidenbach M, Tenne R, Seifert G (2011) New route for stabilization of 1T-WS_2 and MoS_2 phases. J Phys Chem C 115(50):24586–24591
15. Wang H, Lu Z, Xu S, Kong D, Cha JJ, Zheng G, Cui Y (2013) Electrochemical tuning of vertically aligned MoS_2 nanofilms and its application in improving hydrogen evolution reaction. Proc Natl Acad Sci 110(49):19701–19706
16. Kan M, Wang JY, Li XW, Zhang SH, Li YW, Kawazoe Y, Jena P (2014) Structures and phase transition of a MoS_2 monolayer. J Phys Chem C 118(3):1515–1522
17. Cheng Y, Nie A, Zhang Q, Gan LY, Shahbazian-Yassar R, Schwingenschlogl U (2014) Origin of the phase transition in lithiated molybdenum disulfide. ACS Nano 8(11):11447–11453
18. Nasr Esfahani D, Leenaerts O, Sahin H, Partoens B, Peeters FM (2015) Structural transitions in monolayer MoS_2 by lithium adsorption. J Phys Chem C 119(19):10602–10609
19. Pandey M, Bothra P, Pati SK (2016) Phase transition of MoS2 bilayer structures. J Phys Chem C 120(7):3776–3780
20. Du G, Guo Z, Wang S, Zeng R, Chen Z, Liu H (2010) Superior stability and high capacity of restacked molybdenum disulfide as anode material for lithium ion batteries. Chem Commun 46(7):1106–1108
21. Stephenson T, Li Z, Olsen B, Mitlin D (2014) Lithium ion battery applications of molybdenum disulfide (MoS_2) nanocomposites. Energy Environ Sci 7(1): 209–231
22. Mortazavi M, Wang C, Deng J, Shenoy VB, Medhekar NV (2014) Ab initio characterization of layered MoS_2 as anode for sodium-ion batteries. J Power Sources 268:279–286
23. Gao P, Wang L, Zhang Y, Huang Y, Liu K (2015) Atomic-scale probing of the dynamics of sodium transport and intercalation-induced phase transformations in MoS_2. ACS Nano 9(11):11296–11301
24. Kresse G, Furthmüller J (1996) Efficiency of ab-initio total energy calculations for metals and semiconductors using a plane-wave basis set. Comput Mater Sci 6(1):15–50
25. Perdew JP, Burke K, Ernzerhof M (1996) Generalized gradient approximation made simple. Phys Rev Lett 77(18):3865
26. Rastogi P, Kumar S, Bhowmick S, Agarwal A, Chauhan YS (2014) Doping strategies for monolayer MoS_2 via surface adsorption: a systematic study. J Phys Chem C 118(51):30309–30314
27. Li XD, Fang YM, Wu SQ, Zhu ZZ (2015) Adsorption of alkali, alkaline-earth, simple and 3d transition metal, and nonmetal atoms on monolayer MoS_2. AIP Adv 5(5):057143
28. Su J, Pei Y, Yang Z, Wang X (2014) Ab initio study of graphene-like monolayer molybdenum disulfide as a promising anode material for rechargeable sodium ion batteries. RSC Adv 4(81):43183–43188
29. Aydinol MK, Kohan AF, Ceder G, Cho K, Joannopoulos J (1997) Ab initio study of lithium intercalation in metal oxides and metal dichalcogenides. Phys Rev B 56(3):1354
30. Lebegue S, Eriksson O (2009) Electronic structure of two-dimensional crystals from ab initio theory. Phys Rev B 79(11):115409